

RESEARCH ARTICLE

10.1002/2014JD021854

Key Points:

- Tropospheric ozone over western India analyzed using FLEXPART retroplume model
- Tropospheric ozone affected by both local and long-range transport
- Lowest ozone levels observed during fall in the height range of 10–14 km

Correspondence to:

S. Lal,
shyam@prl.res.in

Citation:

Lal, S., S. Venkataramani, N. Chandra, O. R. Cooper, J. Brioude, and M. Naja (2014), Transport effects on the vertical distribution of tropospheric ozone over western India, *J. Geophys. Res. Atmos.*, 119, 10,012–10,026, doi:10.1002/2014JD021854.

Received 3 APR 2014

Accepted 23 JUL 2014

Accepted article online 28 JUL 2014

Published online 20 AUG 2014

Transport effects on the vertical distribution of tropospheric ozone over western India

S. Lal¹, S. Venkataramani¹, N. Chandra^{1,2}, O. R. Cooper^{3,4}, J. Brioude^{3,4,5}, and M. Naja⁶

¹Physical Research Laboratory, Ahmedabad, India, ²Indian Institute of Technology, Gandhinagar, India, ³Cooperative Institute for Research in Environmental Sciences, University of Colorado, Boulder, Colorado, USA, ⁴NOAA Earth System Research Laboratory, Boulder, Colorado, USA, ⁵Laboratoire de l'Atmosphère et des Cyclones, CNRS-Meteo France-Universite, La Reunion, La Reunion, France, ⁶Aryabhata Research Institute of Observational Sciences, Nainital, India

Abstract In situ tropospheric ozone measurements by balloon-borne electrochemical concentration cell (ECC) sensors above Ahmedabad in western India from May 2003 to July 2007 are presented, along with an analysis of the transport processes responsible for the observed vertical ozone distribution. This analysis is supported by 12 day back trajectory calculations using the FLEXPART Lagrangian particle dispersion model. Lowest ozone (~20 ppbv) is observed near the surface during September at the end of the Asian summer monsoon season. Average midtropospheric (5–10 km above sea level) ozone is greatest (70–75 ppbv) during April–June and lowest (40–50 ppbv) during winter. Ozone variability is greatest in the upper troposphere with higher ozone during March–May. The FLEXPART retroplume results show that the free tropospheric vertical ozone distribution above this location is affected by long-range transport from the direction of North Africa and North America. Ozone levels are also affected by transport from the stratosphere particularly during March–April. The lower tropospheric (<3 km) ozone distribution during the Asian summer monsoon is affected by transport from the Indian Ocean via the east coast of Africa and the Arabian Sea. Influence from deep convection in the upper troposphere confined over central Asia has been simulated by FLEXPART. Lower ozone levels are observed during August–November than in any other season at 10–14 km above sea level. These in situ observations are in contrast to other studies based on satellite data which show that the lowest ozone values at these altitudes occur during the Asian summer monsoon.

1. Introduction

Ozone in the troposphere plays crucial roles as an oxidant and as a greenhouse gas. It is the major source of the highly reactive OH radicals in the troposphere, which control oxidation processes as well as act as a cleaning agent by controlling the abundance of many trace gases, particularly hydrocarbons [Monks *et al.*, 2009]. Ozone traps the outgoing long-wave radiation at 9.6 μm , and its contribution to radiative forcing is significant next to CO₂ and CH₄ [Gauss *et al.*, 2003; Stevenson *et al.*, 2012; Intergovernmental Panel on Climate Change, 2013]. The efficiency of this radiative forcing is greater at higher altitudes in the troposphere [Lacis *et al.*, 1990; Gauss *et al.*, 2003]. Ozone in the troposphere is also a pollutant that impacts air quality [The Royal Society, 2008; Ravishankara *et al.*, 2012].

Ozone in the troposphere is either transported from the stratosphere or produced photochemically from pollutants emitted by anthropogenic and natural processes [Crutzen, 1995]. The first source is mostly dominant in the upper troposphere while the latter plays a major role in the lower troposphere. The lifetime of ozone varies from hours near the surface to months in the free troposphere. Since its lifetime is high in the middle and upper troposphere, ozone (and some of its precursors) can be transported over long distances [Lelieveld *et al.*, 2002; Liu *et al.*, 2003; Lawrence and Lelieveld, 2010; Dentener *et al.*, 2011]. Tropospheric ozone above the U.S. is affected by South and East Asian anthropogenic emissions due to the prevailing westerly winds at midlatitudes [Cooper *et al.*, 2005a, 2010; Lin *et al.*, 2012]. However, Asia is also influenced by European emissions [Wild *et al.*, 2004; Naja and Akimoto, 2004]. Particularly relevant to this analysis, a study of ozone profiles in the lower troposphere shows that Ahmedabad in western India is affected by transport from Southern Europe and North Africa [Srivastava *et al.*, 2012].

South and East Asian countries are experiencing strong industrial and economic growth leading to increasing emissions of pollutants, many of which are ozone precursors [Akimoto, 2003; Streets *et al.*, 2003; Gurjar *et al.*, 2004; Lal *et al.*, 2004; Olivier *et al.*, 2005; Ohara *et al.*, 2007]. Because the tropical regions of Asia are strongly

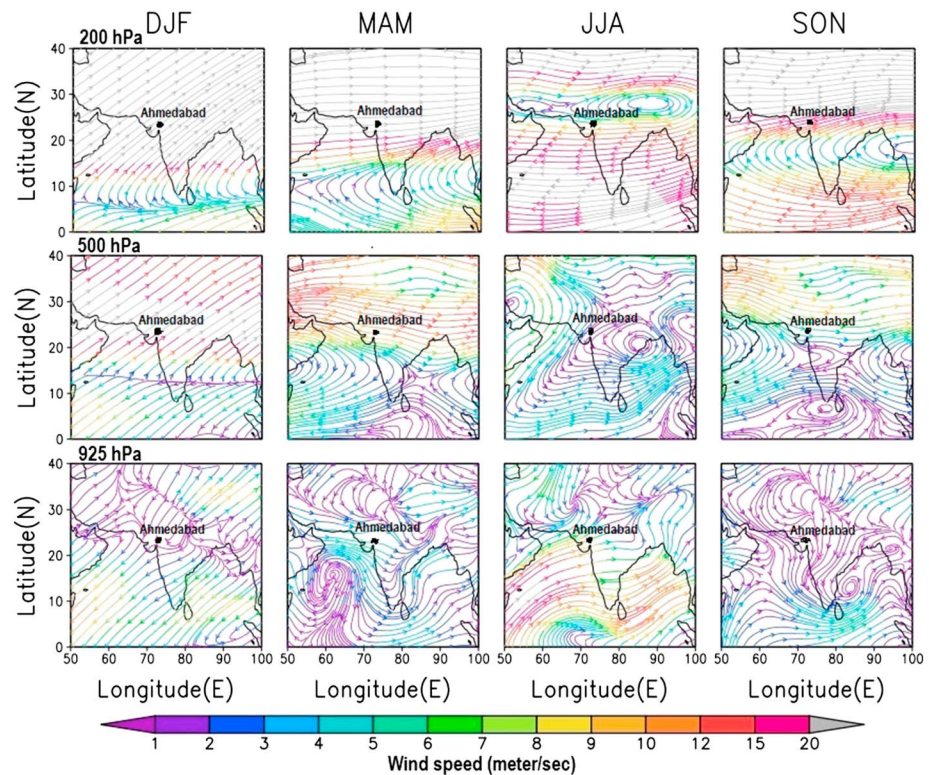


Figure 1. Average streamlines based on NCEP reanalysis data during winter (DJF), spring (MAM), monsoon (JJA), and fall (SON) seasons at 925, 500, and 200 hPa. The color bar code at the bottom is wind speed (m s^{-1}).

affected by deep convection [Emanuel, 1994], the region’s ozone and ozone precursors can be lofted to the middle and upper troposphere, with subsequent advection across great distances [Kley et al., 1997; Kar et al., 2004; Folkins and Martin, 2005]. During the last decade, enhanced pollution in the upper troposphere has been observed over Asia and the Middle East due to widespread deep convection during the summer monsoon period. The polluted convective outflow can be confined over this region by the strong anticyclonic circulation associated with the Asian summer monsoon [Gettelman et al., 2004; Randel and Park, 2006; Randel et al., 2010; Park et al., 2007; Worden et al., 2009; Liu et al., 2009, 2011; Barret et al., 2011].

India is a developing country located in the tropics and subtropics with over 1 billion citizens. Hence, the atmosphere over this region is strongly impacted by increasing emissions of pollutants due to anthropogenic activities, along with intense sunlight and high water vapor content. However, studies related to tropospheric ozone are very limited for the Indian region despite its importance for the Northern Hemisphere budgets of ozone and particulate matter [Lawrence and Lelieveld, 2010], with many of these studies based on satellite data [Fishman et al., 2003; Saraf and Beig, 2004; Beig and Singh, 2007; Fadnavis et al., 2010]. Here we present an analysis of tropospheric ozone based on in situ ozonesonde observations from May 2003 to July 2007 to improve the scientific community’s understanding of the ozone distribution above western India and the transport processes that modulate its abundance.

2. Location and Meteorology

Ahmedabad (23.03°N, 72.54°E, 50 m above mean sea level (amsl)) (see Figure 1) is an urban center in central west India, with a population of 5.6 million that has increased by about 20% in the last decade [http://www.censusindia.gov.in]. The Thar Desert is located to the northwest (about 500 km) and the Arabian Sea to the southwest with the closest shores being 100 km to the south and 400 km to the west. Physical Research Laboratory (PRL), where the ozonesondes were launched, is located on the western side of the city. Textile mills and pharmaceutical production facilities are located in and around the city with most industries in the eastern and northern regions, about 15–20 km from PRL. In addition, a 400 MW coal-fired power plant is

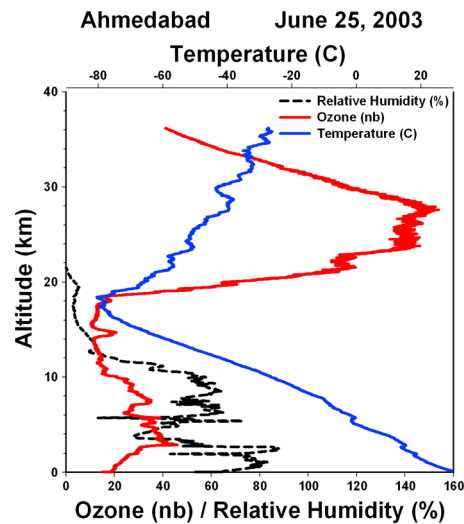


Figure 2. Ozone, temperature, and relative humidity profiles as observed from a balloon ascent on 25 June 2003 above Ahmedabad.

located approximately 10 km to the northeast. Ahmedabad has a large number (about 2.5 million) of automobiles, which are increasing at the rate of about 10% per year.

Ahmedabad has a hot semiarid climate. The climate is dry except during the summer monsoon season. The weather is hot from April to June, while winds during December–February bring milder conditions. The monthly average surface temperature is in the range of 28°C to 35°C during summer and 20°C to 25°C during the winter months of November to February. The southwest Asian summer monsoon produces a humid climate from mid-June to mid-September with an average annual rainfall of about 750 mm. Most rainfall over Ahmedabad occurs during July (~43%) and August (~27%).

The average wind patterns based on National Centers for Environmental Prediction (NCEP) reanalysis data for December-January- February (DJF), March-April-May (MAM), June-July-August (JJA), and September-October-November (SON) on the 925, 500, and 200 hPa surfaces are shown in Figure 1. The winds over Ahmedabad at 925 hPa are

northeasterly during winter (DJF), westerly during spring (MAM), southwesterly during the summer monsoon (JJA), and northwesterly during autumn (SON).

The streamlines at 500 hPa are southwesterly during DJF, westerly during MAM, northeasterly during JJA, and again westerly during SON. At 200 hPa, the winds are stronger and southwesterly during DJF, westerly during MAM, and again southwesterly during SON. However, the winds are easterly during the summer monsoon months with an anticyclone pattern centered over the Himalaya and extending to the Middle East.

3. Techniques

3.1. Ozone and Meteorological Soundings

Vertical profiles of ozone, pressure, humidity, and temperature were measured using balloon-borne ozonesondes coupled to radiosondes. Each ozonesonde consists of a Teflon pump, an ozone sensing electrochemical concentration cell (ECC) [Komhyr and Harris, 1971], and an electronic interface board. The ECC is comprised of Teflon cathode and anode chambers containing platinum electrodes immersed in KI solutions of two different concentrations thereby providing a potential difference to collect the electrons produced in the cathode chamber from the reaction between the KI solution and ozone present in the ambient atmosphere. Its accuracy is $\pm 5\text{--}10\%$ up to 30 km altitude [Smit *et al.*, 2007]. The Vaisala RS-80 radiosonde consists of capacitance-based temperature, humidity, and pressure sensors. The temperature and pressure sensors have accuracies below 20 km of $\pm 0.3^\circ\text{C}$ and ± 0.5 hPa, respectively. The heights are calculated based on the observed pressure and are above mean sea level (amsl). However, the humidity sensor has an accuracy of about $\pm 2\%$ near the ground which decreases to $\pm 15\text{--}30\%$ in the 5–15 km altitude range [Kley *et al.*, 1997].

Balloon soundings carrying an ozonesonde and a radiosonde were made from the terrace of PRL once every 2 weeks between 9:30 and 10:30 A.M. Indian Standard Time (IST) (UTC + 5.5 h). Some of these sondes also carried a GPS, which provided winds in addition to the position information. The exact launch time depended on clearance from the Air Traffic Control of the local airport. The first flight was made on 7 May 2003 and the last on 11 July 2007. There were breaks in between due to technical problems or due to other campaigns. A total of 83 ozonesondes were launched during this period. The balloons reached a maximum altitude of 30 to 33 km with an average ascent rate of about 250 m min^{-1} . The instruments fell mostly within 150 km around the launch site, and some of the ozone sensors were recovered and were flown again after proper cleaning, charging, and testing.

Typical vertical distributions of air temperature, relative humidity, and ozone are shown in Figure 2. The humidity profile is shown up to about 20 km, but errors are large above 10 km. The figure shows structures in

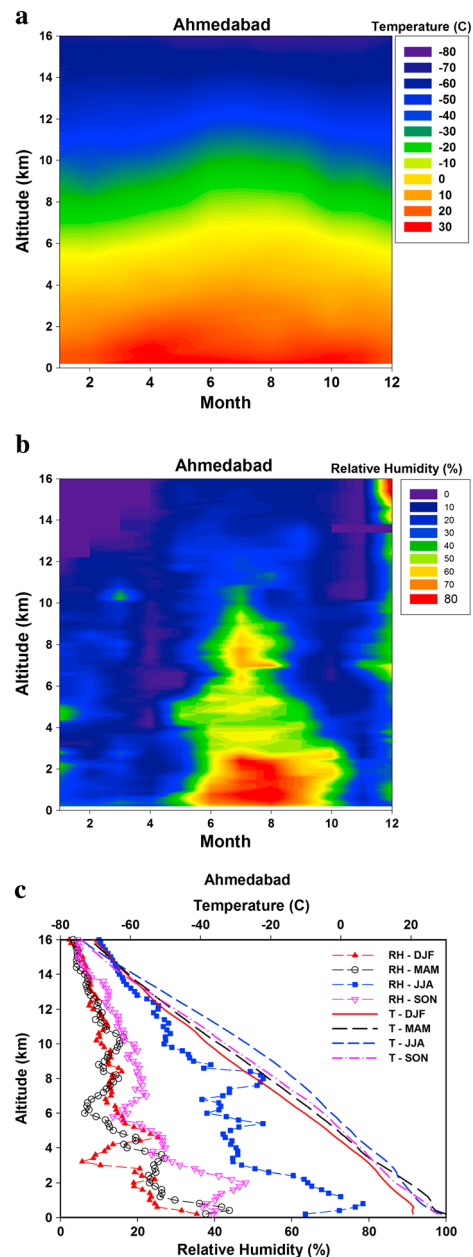


Figure 3. (a) Average temperature, (b) relative humidity during different months, and (c) average seasonal profiles of both observed from the balloon ascents above Ahmedabad during 2003–2007.

trajectory particles is folded with an anthropogenic NO_x emission inventory to quantify the amount of anthropogenic NO_x emitted into the air mass represented by the retroplume [Stohl *et al.*, 2003a, 2003b]. The NO_x emission inventory used in this study is the EDGARv4.1 2005 annual data set, which estimates anthropogenic NO_x emissions on land [Olivier *et al.*, 2005]. International shipping NO_x emissions are from the University of Delaware 2001 inventory [Corbett and Koehler, 2003]. Monthly biomass burning emissions were provided by the Global Fire Emission Database (GFED) version 3 (<http://www.globalfiredata.org>) [van der Werf *et al.*, 2010]. With this technique, the quantity of NO_x emitted into each retroplume from several source regions (India, Southeast Asia, China, Japan-Korea, central Asia, Middle East, Africa, Europe, North America, and South America) was tabulated. The NO_x tracer has no chemical or depositional removal processes and is

the humidity profile and often corresponding changes in temperature. The ozone profile also shows variability sometimes linked to changes in humidity and temperature. The ozone partial pressure increases rapidly around 18 km, peaks around 28 km, and decreases above this altitude.

3.2. Lagrangian Dispersion Model

The FLEXPART Lagrangian particle dispersion model (version 8.1) [Stohl *et al.*, 2005] was used to simulate the 12 day transport history of each ozonesonde profile at 200 m intervals. The model calculates the trajectories of a multitude of particles and was driven by ERA-interim global wind fields, with a temporal resolution of 6 h (analyses at 0000, 0600, 1200, and 1800 UTC), horizontal resolution of $0.7^\circ \times 0.7^\circ$, and 37 pressure levels. Particles are transported both by the resolved winds and parameterized subgrid motions, including a vertical deep convection scheme.

To determine the transport history of each ozone measurement, a retroplume was calculated (see Cooper *et al.* [2005a, 2005b] for a detailed illustration of the method) consisting of 40,000 back trajectory particles released from a box surrounding the location and time of each measurement (1 h duration; 10 km \times 10 km \times 200 m box) and advected backward in time over a 12 day period. Retroplume distributions were output in 1 day intervals on a $2^\circ \times 2^\circ$ output grid covering the globe, with a $0.5^\circ \times 0.5^\circ$ nested grid over India. FLEXPART outputs the retroplumes in units of $\text{s kg}^{-1} \text{m}^3$, which is the residence time of the plume per grid cell divided by the air density. The residence of each retroplume is calculated for the 300 m layer of the atmosphere adjacent to the Earth's surface where the air would pick up surface emissions (known as the footprint layer). For simplicity this specific volume weighted residence time is hereafter referred to as the retroplume residence time.

The dispersion of a retroplume backward in time indicates the likely source regions of the ozone precursors (or stratospheric intrusions) that contributed to the measured ozone but over the previous 12 days. This is especially true of the so-called footprint layer which is the 300 m layer adjacent to the Earth's surface. For plumes passing through this layer, the residence time of the back

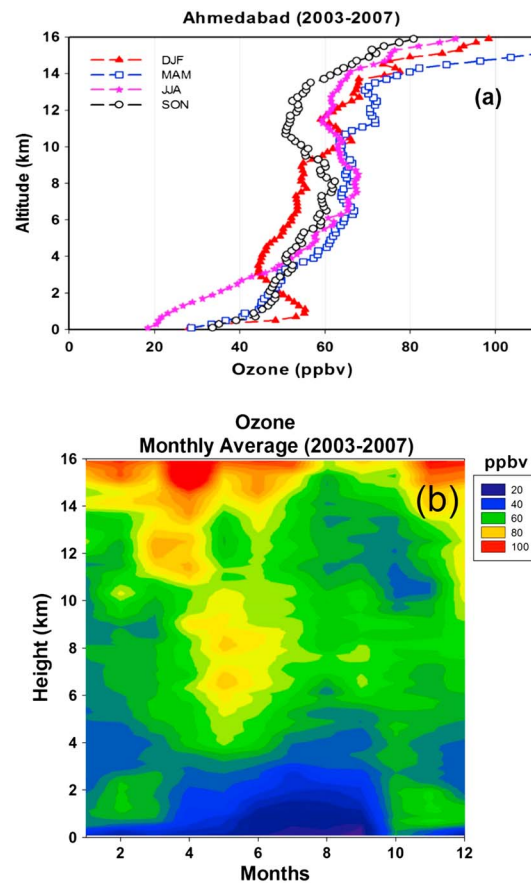


Figure 4. (a) Average ozone mixing ratios (ppbv) during different seasons and (b) during different months observed from the balloon ascents above Ahmedabad during 2003–2007.

temperatures at 3–15 km are observed during the summer monsoon season (JJA). The lapse rates vary widely below about 4 km in the planetary boundary layer, but between 4 km and 15 km, they are mostly in the range of -8 to $-5^{\circ}\text{C}/\text{km}$. The tropopause is observed to be in the 16–18 km range.

Relative humidity varies widely with altitude and from month to month and is at a maximum during the summer monsoon (JJA) and lower during winter and spring (Figures 3b and 3c). The average monthly minimum at the surface occurs in November ($\sim 25\%$), and the maximum occurs in July ($\sim 69\%$). The greatest values extend up to about 10 km during the peak monsoon month of July. Occasionally, higher relative humidity is also observed in December/January due to the winter monsoon.

4.2. Ozone Distribution in the Troposphere

The average seasonal profiles of ozone mixing ratios are shown in Figure 4a. Ozone increases rapidly with altitude in the lower troposphere (below about 1 km height) during winter (DJF). Average ozone is about 28 ppbv near the surface but increases to about 56 ppbv near 1 km. This could be due to a shallow boundary layer during this season and loss near the surface due to dry deposition or destruction by NO. Above 1 km, ozone decreases to about 45 ppbv at 3.5 km; above this altitude, ozone increases slowly throughout the entire troposphere. In the middle troposphere (4 to 10 km, height), average ozone is highest in spring (MAM) and the summer monsoon (JJA) seasons and lowest in the winter season (DJF). Ozone is lowest (~ 18 ppbv) during the monsoon season (JJA) near the surface and remains low below 3 km. However, at 7 to 9 km, ozone is slightly greater (~ 66 ppbv) in JJA than during MAM. Ozone during autumn (SON) is similar to spring below 3.5 km, but it is lower than all other seasons between 9 and 16 km. The ozone profiles in MAM and SON have sharper increases than in other seasons above 13 km. The average ozone in the upper troposphere (above 10 km height) is highest in spring, particularly in March–April and lowest in autumn (SON). Measurements

treated as a passive tracer. The ERA-Interim analyses contain stratospheric ozone values above the tropopause. We use these gridded values to calculate the quantity of ozone transported from the stratosphere to the location where a retroplume is released. This method involves tagging all retroplume back trajectory particles that originated in the stratosphere and scaling the mass of each particle by the ozone value at its highest altitude in the lower stratosphere. The accuracy of the stratospheric ozone tracer was also assessed using 260 ozonesonde profiles above the U.S. during summer 2004 [Cooper et al., 2005b, 2006]. The result is an upper limit of the estimated stratospheric ozone that was directly transported from the stratosphere to a retroplume release point over the previous 12 days.

4. Results and Discussions

4.1. Temperature and Humidity Variations

The observed average air temperature in the troposphere is shown in Figures 3a and 3c. The average seasonal temperature profiles show minimum surface temperatures of about 20°C in winter (DJF) at the time of morning balloon launches (9:30–10:30 A.M.). Winter temperatures are lower than in all other seasons up to about 15 km. The highest average seasonal surface temperature (about 30°C) is observed in spring (MAM). But at 3–15 km, spring temperatures are lower than during JJA and SON. The highest

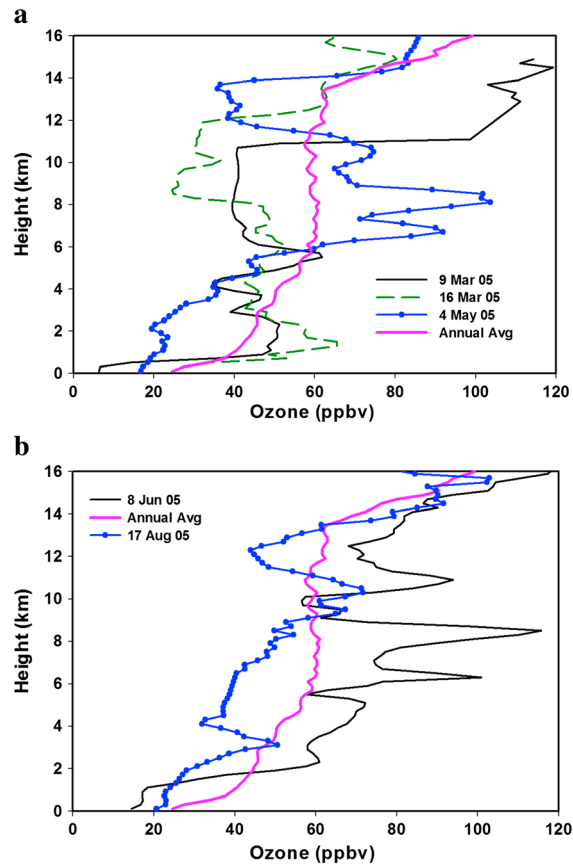


Figure 5. Ozone profiles observed above Ahmedabad on different dates (a) during March–May 2005 and (b) during June–August 2005, along with the annual average profile.

made over Hilo, Hawaii (19.4°N), have a maximum during spring in the free troposphere above 3 km [Cooper *et al.*, 2011]. The present results also show that the highest ozone values in the free troposphere above Ahmedabad occur in spring. The lowest ozone in the 10–12 km range is observed in SON at both the locations. However, overall, ozone values are greater above Ahmedabad in all seasons, when compared with observations at Hilo.

Variation of ozone in the troposphere based on average monthly values at 200 m intervals using all balloon flights during 2003–2007 is shown in Figure 4b. Ozone mixing ratios are lowest below about 2 km during April to September. This is the period when the winds are from the southwest, bringing air from the marine regions of the Indian Ocean and the Arabian Sea. Higher ozone mixing ratios are observed from October to March below about 2 km. However, lower ozone levels are observed during these months between 3 and 5 km. In the midtroposphere, ozone values as high as 70–80 ppbv are observed in May–June at 6–9 km. The two higher ozone spots seen in May at 6 and 8 km heights are caused by relatively higher ozone peaks observed on 30 May 2007 and 4 May 2005, respectively. The FLEXPART analysis indicated that these higher ozone containing air masses came from higher latitudes on these 2 days. Lower ozone in the upper troposphere above 10 km is observed

during August to November. High ozone in the upper troposphere is observed throughout the year except during August to October. Stratospheric intrusions penetrate deeper into the troposphere during March–April.

The average seasonal profiles discussed above show little vertical variability. However, there is large variability in the vertical tropospheric ozone distribution from flight to flight. Figures 5a and 5b show individual ozone profiles on several days during different months of 2005. The annual average profile is also shown for comparison. Large variability occurs not only in the upper troposphere but throughout the troposphere. Figure 5a shows ozone profiles during March and May 2005. Surface level ozone was observed to be lowest (only about 6 ppbv) on 9 March, but ozone was highest above 11 km (greater than 100 ppbv at 11 km). On the contrary, ozone was highest (~65 ppbv) around 2 km on 16 March but lowest (~30 ppbv) around 11 km. The ozone profile on 4 May shows very high ozone (~105 ppbv) around 8.5 km, while on 16 March it was only about 25 ppbv at the same altitude. Similar sharp peaks with values of 100 and 115 ppbv were observed at 6–9 km on 8 June 2005 (Figure 5b). Such high ozone layers have been observed at other locations also [Newell *et al.*, 1999; Lal *et al.*, 2013].

Figure 6 shows observed monthly average ozone at selected heights covering different regions of the troposphere. The variation of the monthly average tropospheric column ozone estimated from the observed profiles is also shown for a comparison. Ozone mixing ratios at 0.5 km (average of values within ±0.5 km) show large variation with decreasing ozone from 44 ppbv in January to a minimum of 18 ppbv in September. There is a sudden increase in ozone at this height in October with a maximum of 53 ppbv in November. The average ozone values at 4.5, 8.5, and 12.5 km show different patterns than that at 0.5 km. Ozone values at 4.5 and 8.5 km have maxima during April–May with lowest values in January. The variation at 12.5 km shows sharper changes, but the maximum ozone (81 ppbv) is observed in early spring (March–April). Additionally, higher ozone is also seen in winter (December–January). The tropospheric ozone column (TOC) is greatest in

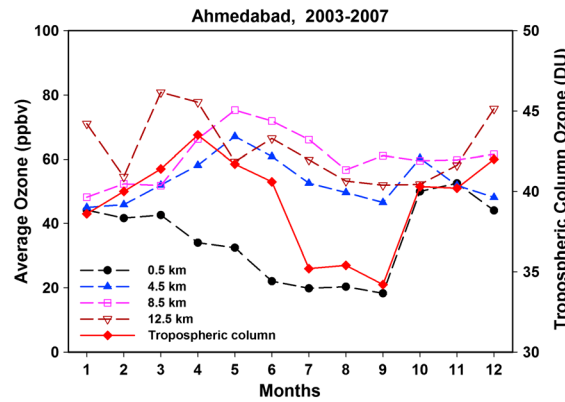


Figure 6. Average ozone during different months and at different heights based on all the balloon ascents made over Ahmedabad during 2003–2007. Variations in the monthly average tropospheric ozone columns are also shown.

April (~44 Dobson unit (DU)) and least (~34–35 DU) during July, August, and September. Sharp increases in TOC are also observed from September to October, as at 0.5 km.

4.3. Residence Times of Air Parcels in Different Global Regions

The FLEXPART retroplume technique [Stohl et al., 2003a, 2003b; Cooper et al., 2005a, 2010] has been used to calculate residence times of air parcels above several regions including India, Southeast Asia, China, Japan-Korea, central Asia, the Middle East, Africa, Europe, North America, and South America (Figure 7).

Figures 8a–8d show the average residence times of the retroplumes released from Ahmedabad over India, Southeast Asia, central Asia, the

Middle East, the Arabian Sea, and other regions of the world for different seasons, expressed as the percent of the total global surface residence time for a retroplume over the previous 12 days. During winter (Figure 8a) in the lowest kilometer of the troposphere (within the planetary boundary layer), the percent residence time over India is about 50% but decreases sharply with altitude. The other major contributions below 4 km are from the Arabian Sea and the Middle East. The contribution from Africa dominates above 4 km, albeit in the range of 20–30%. Other regions contribute in the range of 15–20% except East Asia which is less than 10% above about 8 km. The ozone distribution in this season, after the sharp increase in the first 1 km, decreases up to about 4 km. This is also the height where the residence time over India becomes much less, and the contribution from Africa becomes dominant. In fact, ozone is lower than in any other season in the 3–8 km

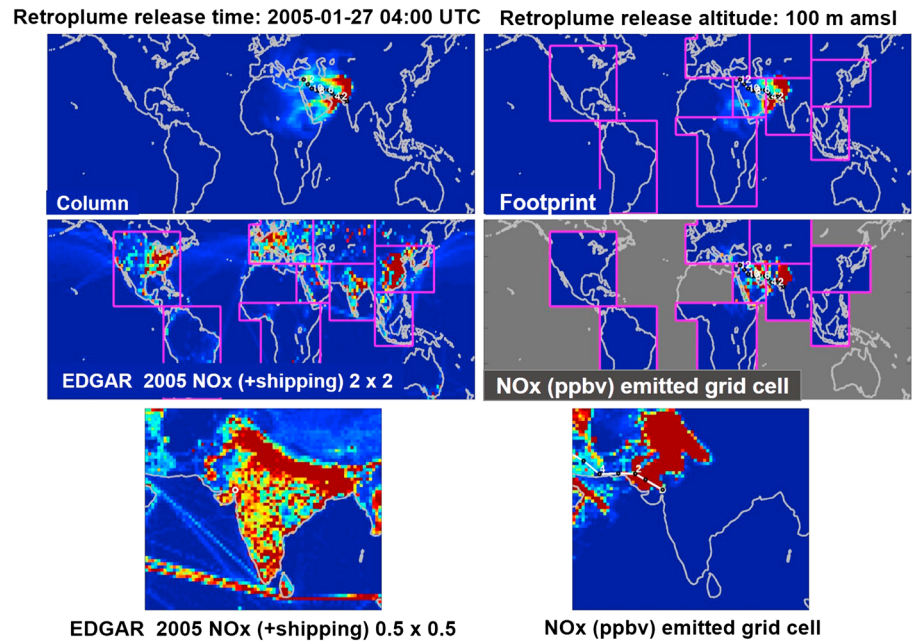


Figure 7. Example of a FLEXPART retroplume released from 100 m above mean sea level (amsl) at Ahmedabad, 4:00 UTC, 27 January 2005. Shown are the retroplume pathway throughout (top left) the entire atmospheric column and (top right) only within the 300 m footprint layer. Magenta boxes outline the regions for which NO_x emissions are totaled. Also shown are (middle left) the 2 × 2° EDGAR NO_x emission inventory and (middle right) the quantity of NO_x emitted into the retroplume from each of the regions of interest. Similarly, the (bottom left) emission inventory and (bottom right) NO_x emitted into the retroplume at 0.5 × 0.5° resolution across South Asia are shown.

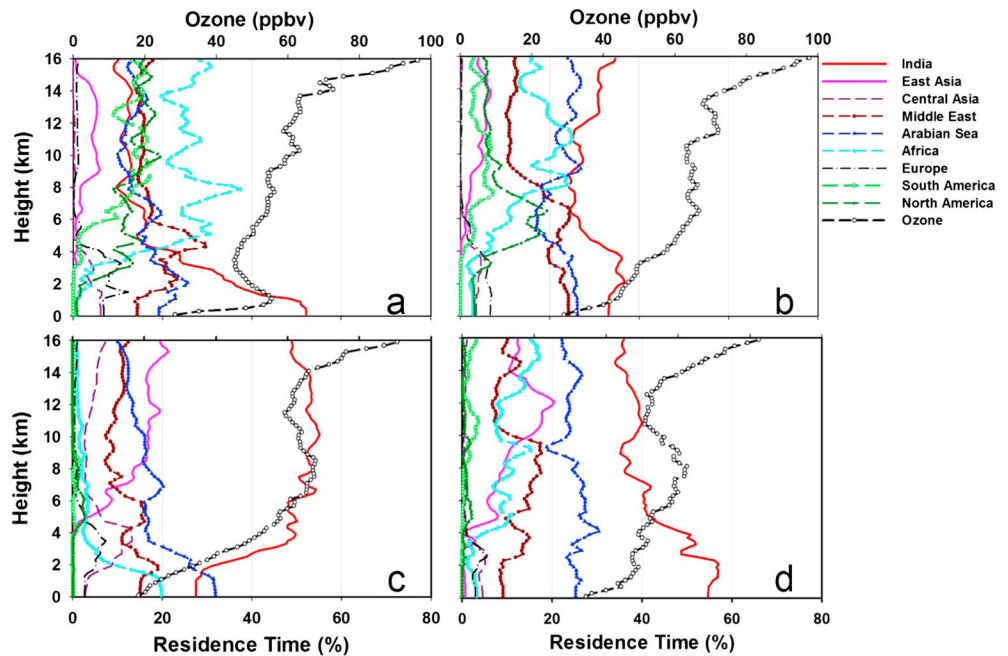


Figure 8. (a–d) Percent residence times over different regions and for different seasons (a- Winter, b- Spring, c- Monsoon, d- Fall) using the average FLEXPART model results for all the balloon flights conducted from Ahmedabad during 2003–2007. Average ozone profiles for each season are also shown.

range, but it is higher above 10 km than in other seasons, such as the summer monsoon and postmonsoon. The dip seen in the monsoon and postmonsoon seasons around 12 km is not seen in winter. This seems to be due to the dominance of air coming from Africa.

The average residence time percentages for the premonsoonal spring season (March, April, and May) are shown in Figure 8b. Compared to winter, the contribution from India (25–35%) has increased in the entire troposphere except in the lowest 1 km. The contribution from the Arabian Sea (mostly in the range of 20–30%) has also increased as compared to winter. On the contrary, the contribution from Africa has decreased and it is less than 25% even in the 8–12 km region. Contributions from other regions have also decreased. Ozone levels have increased at all altitudes above 3 km as compared to winter. This change in residence times, particularly the increase in the contribution from India is associated with increased ozone levels above 3 km.

During the monsoon season (June, July, and August), the percent residence time over India increases sharply above 2 km to approximately 55% in the 6–10 km range (Figure 8c). This is also the region of the troposphere with the highest ozone mixing ratios. The percent residence time over the Arabian Sea is greatest only below 2 km and decreases above this height. Above 8 km, the contribution from East Asia is the second greatest but only reaches 20%. This pattern indicates a strong recirculation of air above India during the summer monsoon that also extends to Southeast Asia, the Middle East, central Asia, and the Arabian Sea.

The percent residence times during the postmonsoon (fall) season (SON) are shown in Figure 8d. Residence times over India dominate throughout the troposphere. Residence times are about 55% in the lower 2 km, much greater than during the monsoon season, but above 4 km, the Indian residence times are much lower than during the monsoon season. The percent residence time over the Arabian Sea decreased to 25% below 3 km but increased (to 25%) above this height in comparison to the monsoon season. The vertical ozone distribution between the monsoon and fall (postmonsoon) seasons is correlated with the residence time above India. Below 4 km, both ozone and the Indian residence time increase from the monsoon to the postmonsoon seasons, with the opposite effect above 4 km.

4.4. Residence Times Over Different Regions

The average monthly residence times are shown in Figure 9 for several regions. The residence time over India is always higher below 2 km except during the monsoon season, with maximum values occurring during

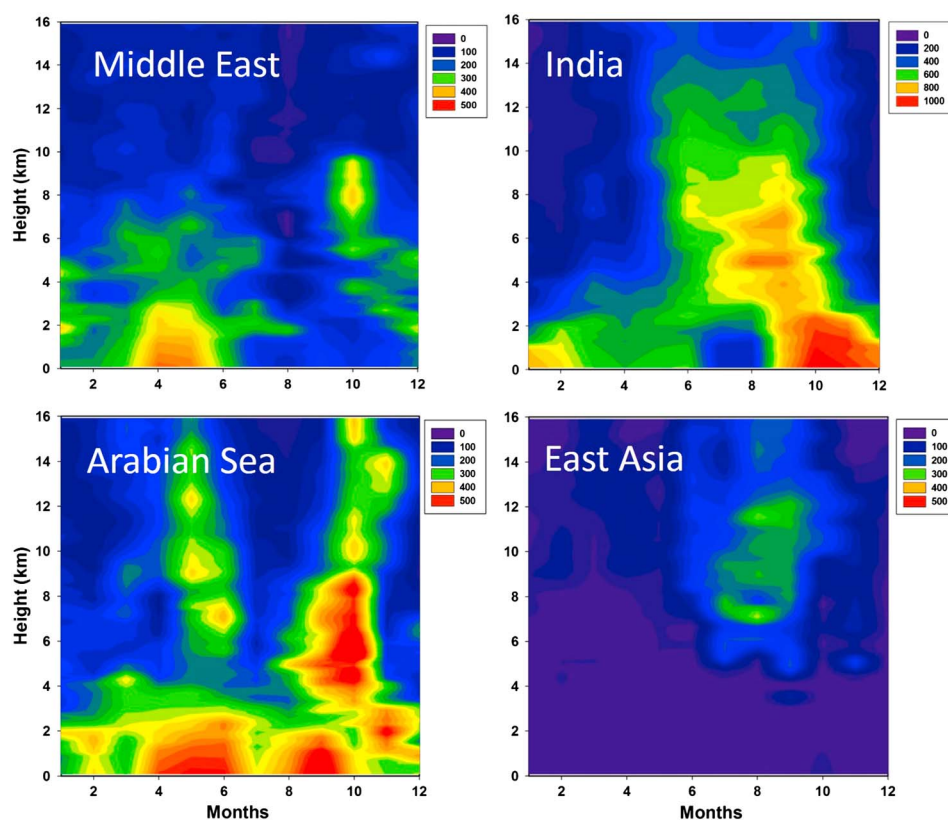


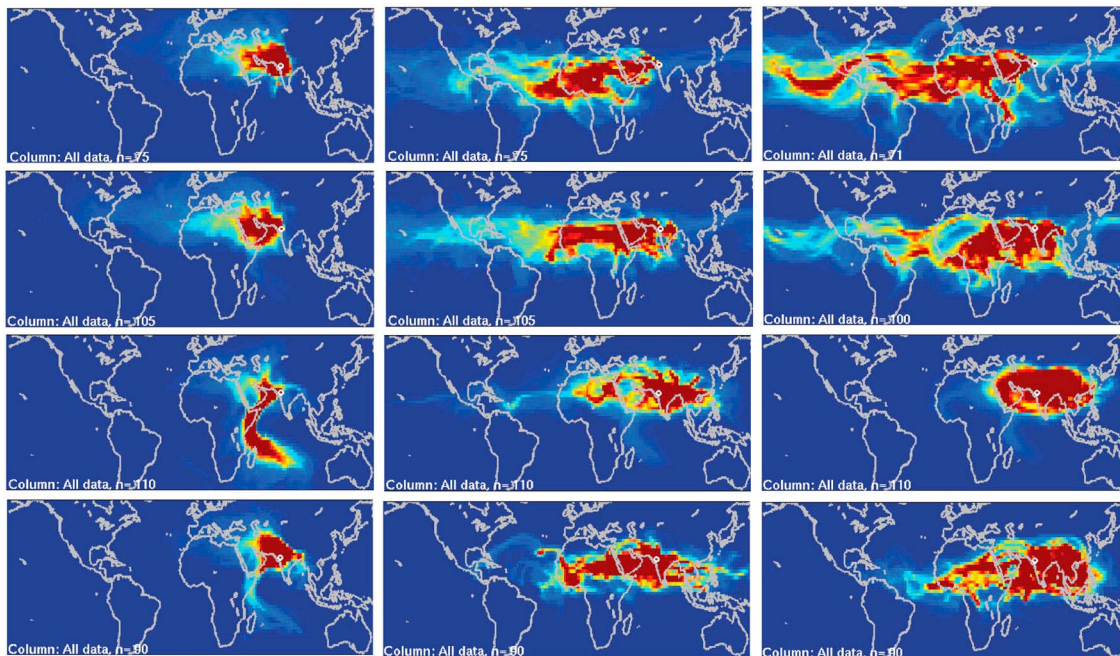
Figure 9. Monthly average residence times (kSec) over major regions using the FLEXPART model results for all the balloon flights conducted from Ahmedabad during 2003–2007. Please note the different scale used for India.

September–December (note the color scale, which is different than over the other regions). The residence time over India is also higher throughout the troposphere from mid-May to mid-October. Note that while the winds in the lower troposphere (<2 km) reach Ahmedabad directly from the Indian Ocean and the Arabian Sea during the peak monsoon period, the weak upper level winds allow air to reside over the Indian region during the previous 12 days. During this period, the retroplumes also show transport from East Asia in the midtroposphere (6–12 km). The East Asian plume is also relatively stronger in the 7–12 km layer and during the July to September period (Figure 9), when the rains over Ahmedabad are heaviest.

Average ozone levels during the monsoon months (JJA) are lowest below about 3 km height as the winds are directly from the Indian Ocean via the Arabian Sea. Even though peak ozone levels occur in May at 5–10 km, ozone remains high during the monsoon and fall months in this height range, while residence times are much higher for the Indian region and East Asian region. This may be due to higher levels of pollutants.

The residence time over the Arabian Sea is more or less higher in the lower troposphere throughout the year, mainly due to proximity to the western Indian region. The residence time over the Arabian Sea is higher during April to October below 2 km. However, there is a dip during July, when the transport pathway from the Indian Ocean touches the African east coast. Ozone is lower throughout this period in this height region. The residence time over this marine region is also higher at the beginning and end of the monsoon period.

March to May experiences hot and dry winds from the Middle East (Figure 9) below about 6 km. This effect is also seen beyond October in the 2–10 km range. This transport pattern only corresponds to lower ozone mixing ratios. As mentioned earlier, July experiences transport from the east coast of Africa below about 2 km. Transport is also from this region above 4 km during October to May. The residence times of retroplumes during October to May above 4 km is dominated by the African region. However, there is also transport from North America especially during March–May in the 4 to 8 km region above Ahmedabad.



Row 1: Dec-Jan-Feb, 0-1 km, 7-8 km, 12-13 km
 Row 2: Mar-Apr-May, 0-1 km, 7-8 km, 12-13 km
 Row 3: Jun-Jul-Aug, 0-1 km, 7-8 km, 12-13 km
 Row 4: Sep-Oct-Nov, 0-1 km, 7-8 km, 12-13 km

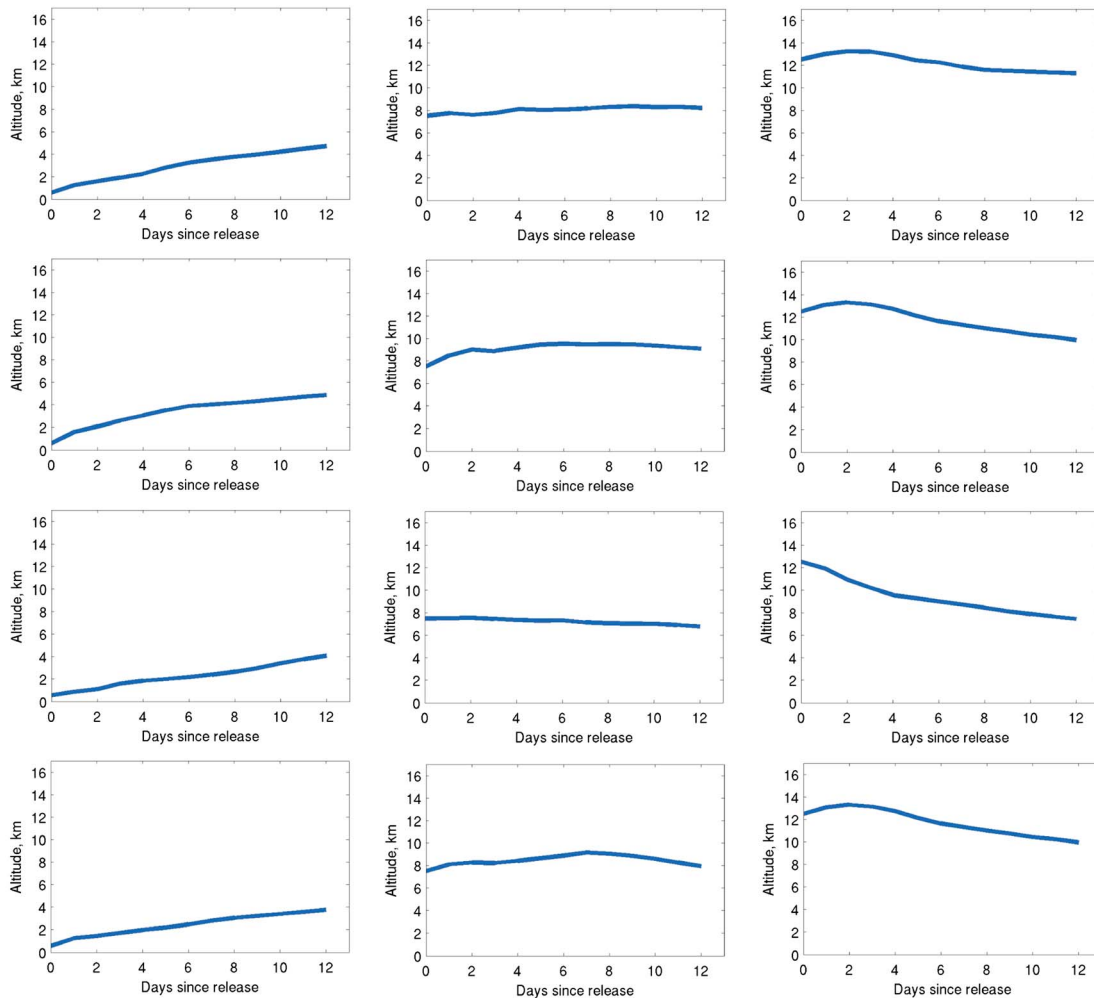
Figure 10a. Composite diagrams showing FLEXPART 12 day retroplumes for (left column) 0–1 km, (middle column) 7–8 km, and (right column) 12–13 km and for (first row) December-January-February, (second row) March-April-May, (third row) June-July-August, and (fourth row) September-October-November. Figure 10a shows transport pathways of the retroplumes during the 12 days prior to release. Retroplumes correspond to the launch times of all balloon ascents during the respective season.

4.5. Long-Range Transport Effects

Many recent studies have documented interregional and intercontinental air pollution transport such as from Asia to North America [Cooper *et al.*, 2010; Lin *et al.*, 2012] and from Asia to Europe [Lawrence and Lelieveld, 2010]. There is also evidence to show that pollutants from Europe, North Africa, etc., also reach East Asia [Newell and Evans, 2000; Naja and Akimoto, 2004] and in particular the South Asian region [Srivastava *et al.*, 2011; Lal *et al.*, 2013]. Transport of pollutants from India to the surrounding marine regions was well documented during Indian Ocean Experiment [Lelieveld *et al.*, 2001] and other campaigns [Srivastava *et al.*, 2011; Lal *et al.*, 2013].

The FLEXPART retroplume analysis over Ahmedabad shows transport of air parcels from nearby regions or from as far away as North America depending upon altitude and season. Figure 10a shows the average transport pathways during winter (DJF), spring (MAM), monsoon (JJA), and postmonsoon/fall (SON) at 0–1 km, 7–8 km, and 12–13 km. The corresponding average heights of the retroplumes during the 12 days prior to the release are shown in Figure 10b. Within the boundary layer (0–1 km), ozone over Ahmedabad is affected in winter mostly by regional transport from the northwest across India, Pakistan, Afghanistan, etc. (Figure 10a). However, in the upper troposphere during this season, ozone can be affected by transport from North Africa, the North Atlantic Ocean, the Central U.S., and the North Pacific Ocean. The corresponding average height of the plumes during this season and during the past 12 days shows descending air from the free troposphere (4–5 km) down to the 0–1 km layer (Figure 10b). However, there is almost no change in the height of the retroplume in the midtroposphere (7–8 km). The pattern in the 12–13 km layer shows a marginal lifting of the air masses. The ozone distribution in spring is affected by dynamics similar to winter at all heights, except that the transport patterns extend farther to the west.

Transport characteristics during the monsoon are very different (Figures 10a and 10b). Ahmedabad is affected by monsoon winds in the 0–1 km range from the Indian Ocean/Arabian Sea via the east coast of



Row 1: Dec-Jan-Feb, 0-1 km, 7-8 km, 12-13 km
 Row 2: Mar-Apr-May, 0-1 km, 7-8 km, 12-13 km
 Row 3: Jun-Jul-Aug, 0-1 km, 7-8 km, 12-13 km
 Row 4: Sep-Oct-Nov, 0-1 km, 7-8 km, 12-13 km

Figure 10b. Same as Figure 10a except for showing average vertical movement of the retroplumes during the 12 days prior to release.

Africa and the western Gulf countries. The midtroposphere is affected by transport from India, East Asia, and to a small extent from North Africa. However, the upper troposphere over Ahmedabad is affected by convective transport from India, the Middle East, and East Asia only. The closed region of recirculation is due to the persistent anticyclonic winds associated with the summer monsoon flow. As in the earlier two seasons, the vertical transport of the average retroplumes shows descent to the 0–1 km layer, marginal lifting to the 7–8 km layer, and stronger convective lifting from below 8 km up to the 12–13 km layer (Figure 10b). In the monsoon season, ozone levels are lower in the upper troposphere compared to winter and spring. But the lowest ozone levels are observed during August–November than in any season at 10–14 km above sea level. These in situ observations are in contrast to other studies based on satellite data which show that the lowest ozone values at these altitudes occur during the Asian summer monsoon due to deep convection [Park et al., 2007, 2009; Randel et al., 2010].

The unique transport pattern during the summer monsoon also produces conditions most conducive for photochemical ozone production in the middle and upper troposphere above India. Figure 11 shows the abundance of the FLEXPART anthropogenic NO_x tracer above Ahmedabad. This passive tracer with a 12 day

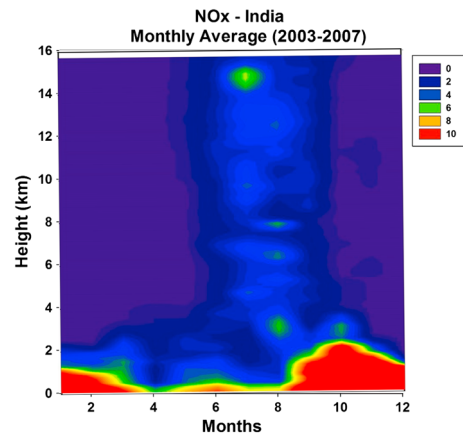


Figure 11. Estimated NO_x (ppbv) over Ahmedabad using the FLEXPART model.

lifetime indicates that relatively fresh anthropogenic emissions are most common in the free troposphere during the summer monsoon. Approximately 80% of the NO_x tracer in the upper troposphere is originated from the surface of India. This result suggests that future changes in Indian emissions would have their greatest impact on the chemical composition of the atmosphere above India during the summer monsoon, a phenomenon that deserves further research, both in terms of chemical transport modeling and in situ observations of chemistry and radiation.

The postmonsoon/fall season is the transition from monsoon to winter conditions and the transport characteristics also change. The vertical transport of the retroplumes at all three levels is similar to those in winter. Ozone levels are lowest above 9 km in this season.

4.6. Stratosphere-Troposphere Exchange

The stratosphere is a significant source of ozone for the middle and upper troposphere as a result of stratosphere-troposphere exchange processes in the extratropics [Stohl *et al.*, 2003a, 2003b]. This flux is greatest in spring [Crutzen, 1995, and references therein] and mainly associated with stratospheric intrusions into the troposphere that form filamentary structures that appear as laminae in ozone profiles [Holton *et al.*, 1995; Stohl *et al.*, 2003a, 2003b]. Stratosphere-to-troposphere transport has also been observed in the tropics involving the transport of stratospheric intrusions from midlatitudes or wave breaking in the subtropics [Baray *et al.*, 1998; Cooper *et al.*, 2005b]. Satellite observations have revealed higher ozone in the upper troposphere above India due to transport from the stratosphere during winter and the premonsoon period [Fadnavis *et al.*, 2010]. Balloon-based measurements have shown stratospheric ozone intrusions in the middle and upper troposphere above the Indian Ocean during February–March 1999 [Zachariasse *et al.*, 2001] and above the Arabian Sea during May 2006 [Lal *et al.*, 2013] and over the central Himalayas [Ojha *et al.*, 2014].

Figure 12 shows the quantity of stratospheric ozone in the troposphere above Ahmedabad according to FLEXPART. The monthly values are averages corresponding to the times of the ozonesonde measurements during 2003–2007. These results show enhanced ozone in March, August, and December in the upper troposphere. Modeled stratospheric contributions are located down to 10 km, with ozone values of about 15–20 ppbv. Extremely high ozone (about 150 ppbv) was observed on 11 April 2007 at about 11.5 km. FLEXPART indicated that this air parcel was transported from the Pacific Ocean via North Africa.

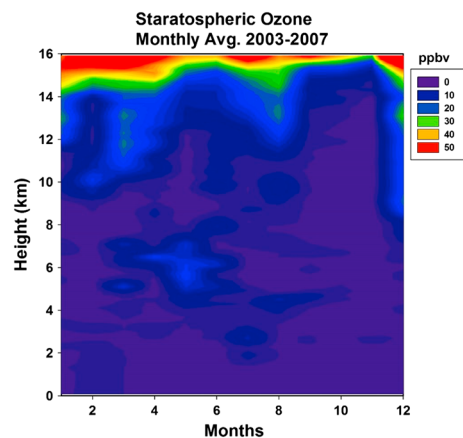


Figure 12. Monthly average contribution of ozone from the stratosphere based on FLEXPART model calculations.

It is interesting to note that even around 5–6 km, FLEXPART indicates stratospheric ozone intrusions during April–June with enhancements up to 15 ppbv. Ozone was observed to be more than 100 ppbv on 30 May 2007 at 6 km, with transport from the upper troposphere and lower stratosphere above the eastern U.S., followed by descent to Ahmedabad via the high-latitude region of Europe.

Livesey *et al.* [2013] observed seasonally enhanced ozone at 215 hPa (~12 km height) over India during March–April using Microwave Limb Sounder (MLS) satellite data. We also observed these high ozone values above Ahmedabad, but in addition, our ozone profiles demonstrate that the enhanced ozone during spring extends down to 6–9 km, a region of the troposphere not visible to MLS.

5. Summary and Conclusions

The vertical distribution of ozone was measured above Ahmedabad using ECC ozonesondes launched twice per month during May 2003 to July 2007 for a total of 83 soundings. The variability of ozone in the troposphere has been studied using these data. The tropospheric column content is at a maximum (44 DU) in April and at a minimum (35 DU) during the monsoon season (July to September). The maximum contribution to this total is associated with altitudes below 4 km. The seasonal average vertical profiles show different features in the three regions of the troposphere: (i) below 4 km (lower troposphere), (ii) between 4 and 10 km (middle troposphere), and (iii) between 10 and 16 km (upper troposphere). In the lower troposphere ozone is greatest during winter (DJF) and lowest during the summer monsoon (JJA). But in the middle troposphere, ozone is at a maximum in spring (MAM) followed by JJA and lowest in winter (DJF). In the upper troposphere, ozone is at a maximum in summer and lowest in the fall (SON). Even though the seasonal ozone profiles do not show much variability, individual profiles show large variability in the middle and upper troposphere, where ozone ranges from 30 ppbv to 110 ppbv.

The FLEXPART retroplume technique was used to calculate residence times of air parcels over several regions such as India, Southeast Asia, China, Japan-Korea, central Asia, Middle East, Africa, Europe, North America, and South America. The residence times and locations of the plumes show very different characteristics. In the lower troposphere (particularly below 2 km) during the summer monsoon, transport is from the Indian Ocean and Arabian Sea via the east coast of Africa. But during winter, the transport pathway is across northwestern India, Pakistan, and Afghanistan. It is interesting to note that in the upper troposphere, the transport pathway is centered over the central Asia region during the summer monsoon but can circle the globe in the zonal direction during winter. This transport pattern can advect stratospheric ozone from higher latitudes to Ahmedabad.

High values of pollutants like CO and low values of ozone have been observed in the upper troposphere–lower stratosphere region during the summer monsoon above North Africa and the Middle East using satellite retrievals (Atmospheric Infrared Sounder and MLS) [Randel and Park, 2006; Park *et al.*, 2007, 2009]. These observations are believed to be due to convectively lifted air from the surface source regions during summer that becomes trapped in the anticyclonic winds in the upper troposphere. Since the convection over India is strong during the monsoon season, lower ozone in the upper troposphere during this season could be due to convective lofting of low ozone air from the lower troposphere.

We observe low ozone over Ahmedabad in the 10–14 km layer from July to November. As mentioned in the previous paragraph, we hypothesize that the low ozone in the UT is due to convective lofting of surface air that is depleted in ozone. Other satellite measurements based on TES retrievals show higher ozone in summer in the middle troposphere above North Africa, the Middle East, and India [Worden *et al.*, 2009; Liu *et al.*, 2009, 2011]. They argue that this midtropospheric enhanced ozone in summer is due to long-range transport of ozone and local production due to enhanced pollutant levels. As mentioned earlier, we find higher ozone in the 6–9 km layer during April–June. Additionally, March–April ozone enhancements detected by MLS are verified here. FLEXPART indicates long-range transport from North America, Africa, and the Middle East to Ahmedabad for this season and altitude range. Hence, different altitudes and seasons have different transport and chemistry in the troposphere.

This is the first detailed analysis of ozone in the full troposphere above western India. These measurements will be useful for the validation of satellite retrievals and model simulations. While this data set gives a broader view of variability of ozone over Ahmedabad and the effects of transport and chemistry, there is a need to understand the various sources and photochemical processes using chemical transport models.

References

- Akimoto, H. (2003), Global air quality and pollution, *Science*, *302*, 1717–1719.
- Baray, J., L. Baray, G. Ancellet, F. G. Taupin, M. Bessafi, S. Baldy, and P. Keckhut (1998), Subtropical tropopause break as a possible stratospheric source of ozone in the tropical troposphere, *J. Atmos. Sol. Terr. Phys.*, *60*, 27–36.
- Barret, B., E. L. Flochmoen, B. Sauvage, E. Pavelin, M. Matricardi, and J. P. Cammas (2011), The detection of post-monsoon tropospheric ozone variability over south Asia using IASI data, *Atmos. Chem. Phys. Discuss.*, *11*, 10,031–10,068.
- Beig, G., and V. Singh (2007), Trends in tropical tropospheric column ozone from satellite data and MOZART model, *Geophys. Res. Lett.*, *34*, L17801, doi:10.1029/2007GL030460.
- Cooper, O. R., et al. (2005a), A springtime comparison of tropospheric ozone and transport pathways on the east and west coasts of the United States, *J. Geophys. Res.*, *110*, D05590, doi:10.1029/2004JD005183.

Acknowledgments

We thank PRL and ISRO GBP for encouraging and supporting this balloon program at PRL. S.L. is grateful to D. Kley and H. Smit for their help in the initial planning of this balloon sounding program at PRL. S.L. is also grateful to A.R. Ravishankara, former Director (now at Colorado State University) of the NOAA Earth System Research Laboratory's Chemical Sciences Division, Boulder, USA, for supporting his stay there to initiate this analysis. We thank Shilpy Gupta, K.S. Modh, T.A. Rajesh, and T.K. Sunilkumar for their support in conducting these balloon flights from Ahmedabad. We thank the anonymous reviewers for their fruitful comments and suggestions, which have greatly improved the paper. We are also grateful to the Editor for his encouragement and support. The EDGARv4.1 global NO_x emissions inventory was provided by European Commission, Joint Research Centre (JRC)/Netherlands Environmental Assessment Agency (PBL): Emission Database for Global Atmospheric Research (EDGAR), release version 4.1 <http://edgar.jrc.ec.europa.eu>, 2010. The international shipping NO_x emission inventory was provided by James Corbett, University of Delaware. Fire NO_x emissions are from the Global Fire Emissions Database version 3 (GFED3).

- Cooper, O. R., et al. (2005b), Direct transport of mid-latitude stratospheric ozone into the lower troposphere and marine boundary layer of the tropical Pacific Ocean, *J. Geophys. Res.*, *110*, D23310, doi:10.1029/2005JD005783.
- Cooper, O. R., et al. (2006), Large upper tropospheric ozone enhancements above midlatitude North America during summer: In situ evidence from the IONS and MOZIC ozone measurement network, *J. Geophys. Res.*, *111*, D24505, doi:10.1029/2006JD007306.
- Cooper, O. R., et al. (2010), Increasing springtime ozone mixing ratios in the free troposphere over western North America, *Nature*, *463*, 344–348.
- Cooper, O. R., et al. (2011), Measurement of western U.S. baseline ozone from the surface to the tropopause and assessment of downwind impact regions, *J. Geophys. Res.*, *116*, D00V03, doi:10.1029/2011JD016095.
- Corbett, J. J., and H. W. Koehler (2003), Updated emissions from ocean shipping, *J. Geophys. Res.*, *108*(D20), 4650, doi:10.1029/2003JD003751.
- Crutzen, P. J. (1995), Ozone in the troposphere, in *Composition, Chemistry, and Climate of the Atmosphere*, edited by H. B. Singh and V. N. Reinhold, New York.
- Dentener, F., T. Keating, and H. Akimoto (Eds.) (2011), Hemispheric transport of air pollution 2010: Part A: Ozone and particulate matter, in *Air Pollution Study*, vol. 17, 278 pp., United Nations Publication, New York.
- Emanuel, K. A. (1994), *Atmospheric Convection*, Oxford Univ. Press, New York.
- Fadnavis, S., T. Chakraborty, and G. Beig (2010), Seasonal stratospheric intrusion of ozone in the upper troposphere over India, *Ann. Geophys.*, *28*, 2149–2159.
- Fishman, J., A. E. Wozniak, and J. K. Creilson (2003), Global distribution of tropospheric ozone from satellite measurements using the empirically corrected tropospheric ozone residual technique: Identification of the regional aspects of air pollution, *Atmos. Chem. Phys.*, *3*, 893–907.
- Folkens, I., and R. V. Martin (2005), The vertical structure of tropical convection and its impact on the budgets of water vapor and ozone, *J. Atmos. Sci.*, *62*, 1560.
- Gauss, M., et al. (2003), Radiative forcing in the 21st century due to ozone changes in the troposphere and the lower stratosphere, *J. Geophys. Res.*, *108*(D9), 4292, doi:10.1029/2002JD002624.
- Gettelman, A., D. E. Kinnison, T. J. Dunkerton, and G. P. Brasseur (2004), Impact of monsoon circulations on the upper troposphere and lower stratosphere, *J. Geophys. Res.*, *109*, D22101, doi:10.1029/2004JD004878.
- Gurjar, B. R., J. A. van Aardenne, J. Lelieveld, and M. Mohan (2004), Emission estimates and trends (1990–2000) for megacity Delhi and implications, *Atmos. Environ.*, *38*, 5663–5681.
- Holton, J. R., P. H. Haynes, M. E. McIntyre, A. R. Douglass, R. B. Rood, and L. Pfister (1995), Stratosphere-troposphere exchange, *Rev. Geophys.*, *33*, 403–439, doi:10.1029/95RG02097.
- Intergovernmental Panel on Climate Change (2013), Working Group I contribution to the IPCC Fifth Assessment Report "Climate Change 2013: The Physical Science Basis", Final Draft Underlying Scientific-Technical Assessment, New York. [Available at <http://www.ipcc.ch>.]
- Kar, J., et al. (2004), Evidence of vertical transport of carbon monoxide from Measurements of Pollution in the Troposphere (MOPITT), *Geophys. Res. Lett.*, *31*, L23105, doi:10.1029/2004GL021128.
- Kley, D., H. G. J. Smit, H. Vomel, H. Grassl, V. Ramanathan, P. J. Crutzen, S. Williams, J. Meywerk, and S. J. Oltmans (1997), Tropospheric water vapour and ozone cross sections in a zonal plane over the central equatorial Pacific, *Q. J. R. Meteorol. Soc.*, *123*, 2009–2040.
- Komhyr, W. D., and T. B. Harris (1971), Development of an ECC ozonesonde, *NOAA Tech. Rep. ERL 200*, APCL 18, Boulder, Colo.
- Lacis, A. A., D. J. Wuebbles, and J. A. Logan (1990), Radiative forcing by changes in the vertical distribution of ozone, *J. Geophys. Res.*, *95*, 9971–9981, doi:10.1029/JD095iD07p09971.
- Lal, S., D. Chand, S. Venkataramani, K. S. Appu, M. Naja, and P. K. Patra (2004), Trends in methane, and sulfur hexafluoride at a tropical coastal site, Thumba (8.6°N, 77°E), in India, *Atmos. Environ.*, *38*(8), 1145–1151.
- Lal, S., S. Venkataramani, S. Srivastava, S. Gupta, C. Mallik, M. Naja, T. Sarangi, Y. B. Acharya, and X. Liu (2013), Transport effects on the vertical distribution of tropospheric ozone over the tropical marine regions surrounding India, *J. Geophys. Res. Atmos.*, *118*, 1513–1524, doi:10.1002/jgrd.50180.
- Lawrence, M. G., and J. Lelieveld (2010), Atmospheric pollutant outflow from southern Asia: A review, *Atmos. Chem. Phys.*, *10*, 11,017–11,096, doi:10.5194/acp-10-11017-2010.
- Lelieveld, J., et al. (2001), The Indian Ocean experiment: Widespread air pollution from South and Southeast Asia, *Science*, *291*, 1031–1036.
- Lelieveld, J., et al. (2002), Global air pollution crossroads over the Mediterranean, *Science*, *294*, 794–799, doi:10.1126/science.1075457.
- Lin, M., et al. (2012), Transport of Asian ozone pollution into surface air over the western United States in spring, *J. Geophys. Res.*, *117*, D00V07, doi:10.1029/2011JD016961.
- Liu, H., D. J. Jacob, I. Bey, R. M. Yantosca, B. N. Duncan, and G. W. Sachse (2003), Transport pathways for Asian pollution outflow over the Pacific: Interannual and seasonal variations, *J. Geophys. Res.*, *108*(D20), 8786, doi:10.1029/2002JD003102.
- Liu, J. J., D. B. A. Jones, J. R. Worden, D. Noone, M. Parrington, and J. Kar (2009), Analysis of the summertime build up of tropospheric ozone abundances over the Middle East and North Africa as observed by the Tropospheric Emission Spectrometer instrument, *J. Geophys. Res.*, *114*, D05304, doi:10.1029/2008JD010993.
- Liu, J. J., D. B. A. Jones, S. Zhang, and J. Kar (2011), Influence of interannual variations in transport on summertime abundances of ozone over the Middle East, *J. Geophys. Res.*, *116*, D20310, doi:10.1029/2011JD016188.
- Livesey, N. J., J. A. Logan, M. L. Santee, J. W. Waters, R. M. Doherty, W. G. Read, L. Froidevaux, and J. H. Jiang (2013), Interrelated variations of O₃, CO and deep convection in the tropical/subtropical upper troposphere observed by the Aura Microwave Limb Sounder (MLS) during 2004–2011, *Atmos. Chem. Phys.*, *13*, 579–598.
- Monks, P. S., et al. (2009), Atmospheric composition change—Global and regional air quality, *Atmos. Environ.*, *43*, 5268–5350.
- Naja, M., and H. Akimoto (2004), Contribution of regional pollution and long-range transport to the Asia-Pacific region: Analysis of long-term ozonesonde data over Japan, *J. Geophys. Res.*, *109*, D21306, doi:10.1029/2004JD004687.
- Newell, R., and M. Evans (2000), Seasonal changes in pollutant transport to the North Pacific: The relative importance of Asian and European sources, *Geophys. Res. Lett.*, *27*, 2509–2512, doi:10.1029/2000GL011550.
- Newell, R. E., V. Thouret, J. Y. N. Cho, P. Stoller, A. Marenco, and H. G. Smit (1999), Ubiquity of quasi-horizontal layers in the troposphere, *Nature*, *398*, 316–319.
- Ohara, T., H. Akimoto, J. Kurokawa, N. Horii, K. Yamaji, X. Yan, and T. Hayasaka (2007), Asian emission inventory for anthropogenic emission sources during the period 1980–2020, *Atmos. Chem. Phys.*, *7*, 4419–4444.
- Ojha, N., M. Naja, T. Sarangi, R. Kumar, P. Bhardwaj, S. Lal, S. Venkataramani, R. Sagar, A. Kumar, and H. C. Chandola (2014), On the processes influencing the vertical distribution of ozone over the central Himalayas: Analysis of yearlong ozonesonde observations, *Atmos. Environ.*, *88*, 201–211.
- Olivier, J. G. J., J. A. van Aardenne, F. Dentener, V. Pagliari, L. N. Ganzeveld, and J. A. H. W. Peters (2005), Recent trends in global greenhouse gas emissions: Regional trends 1970–2000 and spatial distribution of key sources in 2000, *Environ. Sci.*, *2*, 81–99, doi:10.1080/15693430500400345.

- Park, M., W. J. Randel, A. Gettelman, S. T. Massie, and J. H. Jiang (2007), Transport above the Asian summer monsoon anticyclone inferred from Aura Microwave Limb Sounder tracers, *J. Geophys. Res.*, *112*, D16309, doi:10.1029/2006JD008294.
- Park, M., W. J. Randel, L. K. Emmons, and N. J. Livesey (2009), Transport pathways of carbon monoxide in the Asian summer monsoon diagnosed from Model of Ozone and Related Tracers (MOZART), *J. Geophys. Res.*, *114*, D08303, doi:10.1029/2008JD010621.
- Randel, W. J., and M. Park (2006), Deep convective influence on the Asian summer monsoon anticyclone and associated tracer variability observed with Atmospheric Infrared Sounder (AIRS), *J. Geophys. Res.*, *111*, D12314, doi:10.1029/2005JD006490.
- Randel, W. J., M. Park, L. Emmons, D. Kinnison, P. Bernath, K. A. Walker, C. Boone, and H. Pumphrey (2010), Asian monsoon transport of pollution to the stratosphere, *Science*, *328*, 611, doi:10.1126/science.1182274.
- Ravishankara, A. R., J. P. Dawson, and D. A. Winner (2012), New Directions: Adapting air quality management to climate change: A must for planning, *Atmos. Environ.*, *50*, 387–389.
- Saraf, N., and G. Beig (2004), Long-term trends in tropospheric ozone over the Indian tropical region, *Geophys. Res. Lett.*, *31*, L05101, doi:10.1029/2003GL018516.
- Smit, H. G. J., et al. (2007), Assessment of the performance of ECC-ozonesondes under quasi-flight conditions in the environmental simulation chamber: Insights from the Juelich Ozone Sonde Intercomparison Experiment (JOSIE), *J. Geophys. Res.*, *112*, D19306, doi:10.1029/2006JD007308.
- Srivastava, S., S. Lal, S. Venkataramani, S. Gupta, and Y. B. Acharya (2011), Vertical distribution of ozone in the lower troposphere over the Bay of Bengal and the Arabian Sea during ICARB-2006: Effects of continental outflow, *J. Geophys. Res.*, *116*, D13301, doi:10.1029/2010JD015298.
- Srivastava, S., S. Lal, M. Naja, S. Venkataramani, and S. Gupta (2012), Influences of regional pollution and long range transport to western India: Analysis of ozonesonde data, *Atmos. Environ.*, *47*, 174–182.
- Stevenson, D. S., et al. (2012), Tropospheric ozone changes, radiative forcing and attribution to emissions in the Atmospheric Chemistry and Climate Model Intercomparison Project (ACCMIP), *Atmos. Chem. Phys. Discuss.*, *12*, 26,047–26,097.
- Stohl, A., et al. (2003a), Stratosphere-troposphere exchange: A review, and what we have learned from STACCATO, *J. Geophys. Res.*, *108*(D12), 8516, doi:10.1029/2002JD002490.
- Stohl, A., C. Forster, S. Eckhardt, N. Spichtinger, H. Huntrieser, J. Heland, H. Schlager, H. Aufmhoff, F. Arnold, and O. Cooper (2003b), A backward modeling study of intercontinental pollution transport using aircraft measurements, *J. Geophys. Res.*, *108*(D12), 4370, doi:10.1029/2002JD002862.
- Stohl, A., C. Forster, A. Frank, P. Seibert, and G. Wotowa (2005), Technical note: The Lagrangian particle dispersion model FLEXPART version 6.2, *Atmos. Chem. Phys.*, *5*, 2461–2474.
- Streets, D. G., et al. (2003), An inventory of gaseous and primary aerosol emissions in Asia in the year 2000, *J. Geophys. Res.*, *108*(D21), 8809, doi:10.1029/2002JD003093.
- The Royal Society (2008), Ground-level ozone in the 21st century: Future trends, impacts and policy implications, Royal Society policy document 15/08, RS1276, London. [Available at http://royalsociety.org/Report_WF.aspx?pageid57924&terms5ground-level1ozone.]
- van der Werf, G. R., et al. (2010), Global fire emissions and the contribution of deforestation, savanna, forest, agricultural, and peat fires (1997–2009), *Atmos. Chem. Phys.*, *10*, 11,707–11,735, doi:10.5194/acp-10-11707-2010.
- Wild, O., et al. (2004), CTM ozone simulations for spring 2001 over the western Pacific: Regional ozone production and its global impacts, *J. Geophys. Res.*, *109*, D15S02, doi:10.1029/2003JD004041.
- Worden, J., et al. (2009), Observed vertical distribution of tropospheric ozone during the Asian summer time monsoon, *J. Geophys. Res.*, *114*, D13304, doi:10.1029/2008JD010560.
- Zachariasse, M., H. Smit, P. van Velthoven, and H. Kelder (2001), Cross-tropopause and interhemispheric transports into the tropical free troposphere over the Indian Ocean, *J. Geophys. Res.*, *106*(D22), 28,441–28,452, doi:10.1029/2001JD900061.